Supplemntary Infomation: The nanostructure of a lithium glyme solvate ionic liquid at electrified interfaces

Samuel W. Coles,[†] Maksim Mišin,[‡,¶] Susan Perkin,[*,†] Maxim V. Fedorov,[*,§,‡] and Vladislav B. Ivaništšev[*,¶]

†*Department of Chemistry, University of Oxford, South Parks Road, Oxford OX1 3QZ, United Kingdom*

‡*Department of Physics, Scottish Universities Physics Alliance (SUPA), Strathclyde University, John Anderson Building, 107 Rottenrow East, Glasgow G4 0NG, United Kingdom*

¶*Institute of Chemistry, University of Tartu, Ravila 14a, Tartu 50411, Estonia*

§*Skolkovo Institute of Science and Technology, Skolkovo Innovation Center, Moscow 143026 Russia*

E-mail: susan.perkin@chem.ox.ac.uk; m.fedorov@skoltech.ru; vladislav.ivanistsev@ut.ee

Bulk properties [Li(G4)][TFSI] liquids.

In order to evaluate the force field a simulation of bulk [Li(G4)][TFSI] was run for temperatures of both 300 K and 350 K. The simulations were performed using the same Gromacs distribution as for the main paper.[1–7] The simulation was run for a box containing 100 ions, with initial positions generated using the packmol algorithm.[8] After steepest decent energy minimisation the system is annealed from the target temperature to 700K and back again

twice over the course of 2.2 ns. The temperature is maintained using the V-rescale thermostat while pressure is maintained with the Berendsen barostat (due to its greater stability). One equillibration run is then performed at the target temperature followed by a 19 ns production run. For the production run temperature is maintain using the V-rescale thermostat while pressure is maintained with the Parinello-Rahman barostat. The Coulomb and van der Waals cut-offs were set to 1 nm. Long-range electrostatics were performed using the particle mesh Ewald method.[9,10]

Coordination environment

The pair potentials for lithium cations, and glyme oxygen atoms, and bistriflimide oxygen atoms are shown in Fig. S1. While there is a decrease in the magnitude of both peaks between 300K and 350K the two systems can be viewed as highly similar suggesting similar coordination environments at both temperatures.

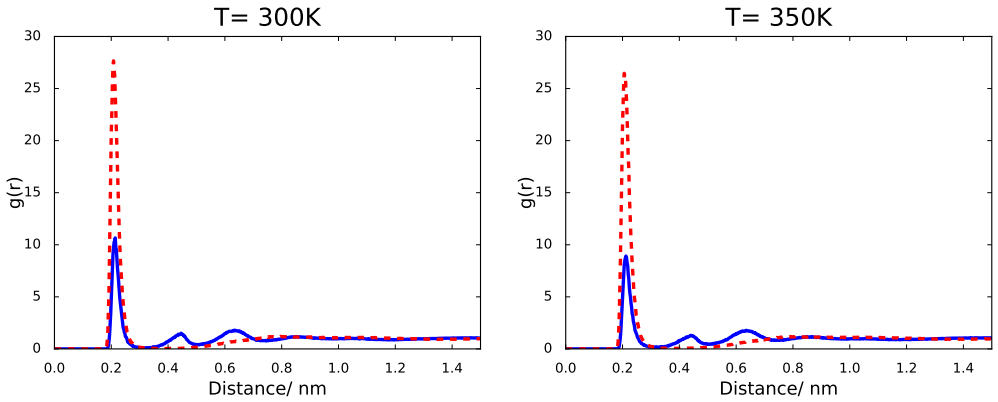

Figure S1: *Plots of the pair potential between lithium ions and glyme oxygens (red dashed line) and lithium and bistriflimide oxygens (solid blue lines). Plots are recorded for two temperatures 300 K and 350 K.*

Transport properties

The mean square displacement of all atoms within the system for temperatures of 300 K, and 350 K are shown in Fig.S2. These plots correspond to diffusion constants of $(0.0014 \times 10^{-5} \mathrm{cm}^2\mathrm{s}^{-1})$

for 300K and (0.0097×10^{-5}cm^{2}s^{-1}) for 350K. As reported by Shimizu *et al.* these diffusion constants are considerably lower than observed for the real liquid.[11] This is not surprising and has been reported for non-polarisable force fields for conventional ionic liquids.[12] As in previous experiments on conventional ionic liquids we run the interfacial simulations at higher temperature (350 K) in order to achieve greater sampling.[13] The results presented in Fig S2 confirm the advantage of doing so for this specific system.

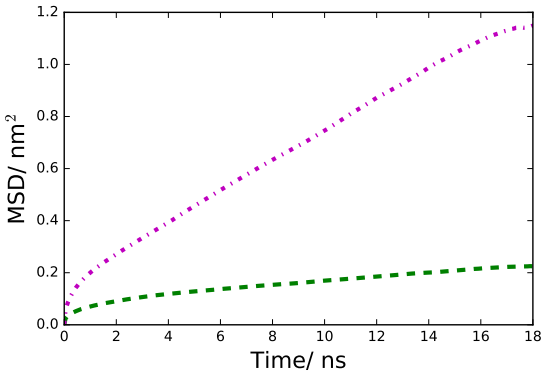

Figure S2: *Plots of the mean square displacement of atoms within the system for temperatures of 300 K (magenta dotted and dashed line), and 350 K (green dashed line.)*

Nanostructure at the positively charged electrode

The simulations performed in this work also provided information regarding the structure observed at the positively charged electrode, see Fig. S3. The structure observed goes through the same transitions as observed in conventional ionic liquids. This can be observed in Fig. S3 by the increasing segregation of ions with increasing charge. In this case the liquid transitions from a mixed monolayer to a charged bilayer structure, as described for conventional ionic liquids in previous reports.[14,15]

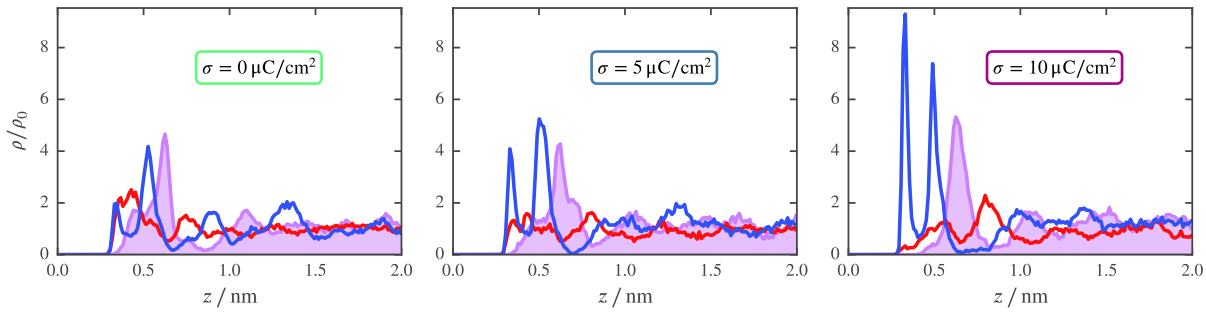

Figure S3: *Relative number density profiles ($\rho(z)/\rho_0$) of bistriflimide nitrogen (blue), Li^+ (purple), and central glyme oxygen (red) . The model electrode with surface charge values of* $0\,\mu C/cm^2$, $+5\,\mu C/cm^2$, *and* $+10\,\mu C/cm^2$ *is situated at* $z = 0$ *nm.*

Potential across the simulated capacitor

The potential at each point within the simulated capacitors used to generate the data reported in both the previous section and in the main paper is shown in Fig. S4. The potential was calculated by integration of charge density within slices of 0.018 nm to obtain an electric field. Followed by a further integration of the electric field in each slice to obtain a plot of changing potential with distance from the negative electrode.

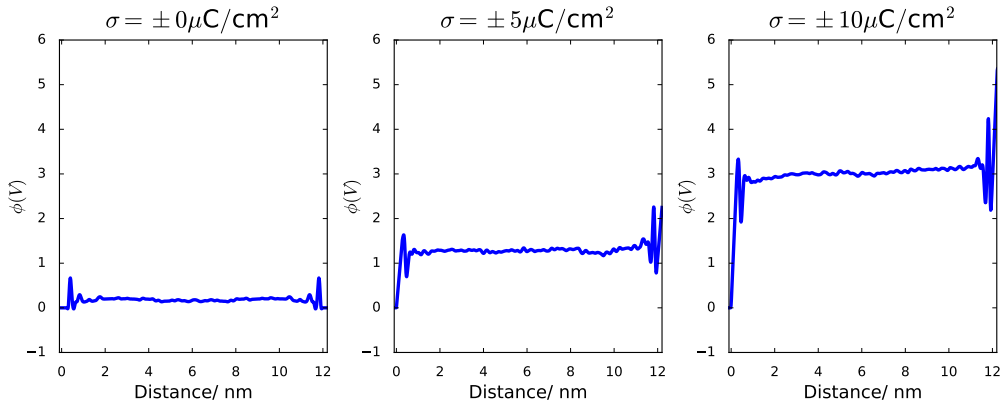

Figure S4: *Plots showing the electrostatic potential with distance from the negative electrode within the simulated capacitors for the three studied surface charges.*

Force Field Parameters

The force field used in this paper was developed by Shimizu *et. al*[11] for their work looking at the bulk structure of this liquid. The partial charges, bonded, and non bonded coefficients are listed below. The force field is based on the CL&P[16] and OPLS-AA[17] force fields widely used in the literature.

Partial Charges

The partial charges of the atoms in the simulations reported are listed below. The experiments are run with value of the relative permitivity (ϵ_r) set to 1.6. The names of atoms are assigned in Fig S5, all hydrogens in the glyme molecule are given the name H, but are not shown in the cartoon .

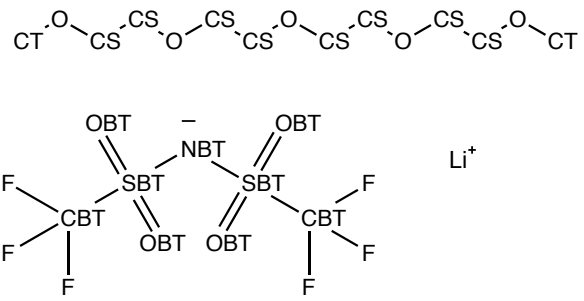

Figure S5: *A cartoon showing the assignment of atom names within the forcefield.*

Atom Name	Charge (e)
NBT	−0.6600
OBT	−0.5300
CBT	0.3500
SBT	1.0200
F	−0.1600
OS	0.5000
CT	0.1375
CS	0.1750
H	0.0375
Li^+	1.0000

Non-bonded Parameters

Non-bonded parameters are listed below. The values for σ and ϵ are listed below, as CT and CS are treated differently only in terms of charge and are hence forth listed as a single entity CG. Standard OPLS-AA combination rules are used for unlike atoms[17]

Atom Name	Mass	σ (nm)	ϵ (kJ mol^{-1})
NBT	14.000	0.325	7.113×10^{-1}
OBT	15.999	0.295	8.786×10^{-1}
CBT	12.011	0.350	2.761×10^{-1}
SBT	32.066	0.355	1.0462
F	18.998	0.295	2.218×10^{-1}
OS	15.999	0.290	5.862×10^{-1}
CG	12.011	0.350	2.762×10^{-1}
H	1.008	0.250	1.255×10^{-1}
Li+	6.941	0.213	7.648×10^{-2}

Bonded Parameters

Bonds

Bonds are modelled using a harmonic potential defined below,

$$V_{\text{bond}}(r_{ij}) = \frac{1}{2}k^b_{ij}(r_{ij} - b_{ij})^2, \tag{1}$$

where b_{ij} is the equilibrium bond length, k^b_{ij} is the force constant, and r_{ij} is the separation between two atoms. The values of these constants are shown below.

i	j	b_{ij} (nm)	k^b_{ij}(kJ mol^{-1}nm^{-2})
NBT	SBT	0.1570	3.137×10^5
SBT	OBT	0.1437	5.331×10^5
SBT	CBT	0.1818	1.950×10^5
CBT	F	0.1323	3.698×10^5
CG	CG	0.1529	7.113×10^5
OS	CG	0.1410	8.786×10^5
CG	H	0.1090	2.761×10^5

Angles

Angles are modelled using a harmonic potential defined below,

$$V_{\text{angle}}(\theta_{ijk}) = \frac{1}{2}k^\theta_{ijk}(\theta_{ijk} - \theta^0_{ijk})^2, \tag{2}$$

where θ^0_{ijk} is the equilibrium angle, k^θ_{ijk} is the force constant, and ${k^\theta_{ijk}}^0$ is the separation between two atoms. The values of these constants are shown below.

i	j	k	θ^0_{ijk} (degrees)	k^θ_{ijk} (kJ mol^{-1} rad^{-2})
NBT	SBT	OBT	113.6	789.0
NBT	SBT	CBT	103.5	764.0
SBT	CBT	F	111.7	694.0
SBT	NBT	SBT	125.6	671.0
CBT	SBT	OBT	102.6	870.0
OBT	SBT	OBT	118.5	969.0
F	CBT	F	107.1	781.0
H	CG	H	107.8	276.1
H	CG	OS	109.5	292.9
CG	OS	CG	109.5	502.4
OS	CG	CG	109.5	418.4
H	CG	CG	110.7	313.8

Dihedrals

The dihedral interactions are modelled using the Ryckaert-Bellemans formulation (which is related to the standard OPLS dihedral formulation),

$$V_{\text{dihedral}}(\phi_{ijkl}) = \sum_{n=0}^{5} C_n(\cos(\phi_{ijkl}))^n, \tag{3}$$

Where C_n is the coefficient for the nth term in the sum.

i	j	k	l	C_0 (kJ mol^{-1})	C_1 (kJ mol^{-1})	C_2 (kJ mol^{-1})	C_3 (KJmol^{-1})
NBT	SBT	CBT	F	0.661	1.983	0.000	−2.644
SBT	NBT	SBT	OBT	−0.008	-0.023	0.000	0.030
SBT	NBT	SBT	CBT	4.369	−21.179	10.420	6.390
OBT	SBT	CBT	F	0.726	2.177	0.000	−2.902
H	CG	CG	H	0.628	1.883	0.000	−2.510
H	CG	CG	OS	0.979	2.937	0.000	−3.916
H	CG	OS	CG	1.590	4.770	0.000	−6.360
CG	CG	OS	CG	1.715	2.845	1.046	−5.607
OS	CG	CG	OS	−1.151	1.151	0.000	0.000

For all dihedral interactions the values of C_4 and C_5 are equal to 0 kJ mol^{-1}

References

(1) Páll, S.; Abraham, M. J.; Kutzner, C.; Hess, B.; Lindahl, E. In *Solving Software Challenges for Exascale*; Markidis, S., Laure, E., Eds.; Springer International Publishing: Cham, 2015; Vol. 8759; pp 3–27.

(2) Abraham, M. J.; Murtola, T.; Schulz, R.; Páll, S.; Smith, J. C.; Hess, B.; Lindahl, E. *SoftwareX* **2015**, *1-2*, 19–25.

(3) Pronk, S.; Páll, S.; Schulz, R.; Larsson, P.; Bjelkmar, P.; Apostolov, R.; Shirts, M. R.; Smith, J. C.; Kasson, P. M.; Spoel, D. v. d.; Hess, B.; Lindahl, E. *Bioinformatics* **2013**, *29*, 845–854.

(4) Hess, B.; Kutzner, C.; van der Spoel, D.; Lindahl, E. *J. Chem. Theory Comput.* **2008**, *4*, 435–447.

(5) Páll, S.; Hess, B. *Computer Physics Communications* **2013**, *184*, 2641–2650.

(6) van der Spoel, D.; Lindahl, E.; Hess, B.; Groenhof, G.; Mark, A. E.; Berendsen, H. J. C. *J. Comput. Chem.* **2005**, *26*, 1701–1718.

(7) Berendsen, H. J. C.; van der Spoel, D.; van Drunen, R. *Comput. Phys. Comm.* **1995**, *91*, 43–56.

(8) Martínez, L.; Andrade, R.; Birgin, E. G.; Martínez, J. M. *J. Comput. Chem.* **2009**, *30*, 2157–2164.

(9) Essmann, U.; Perera, L.; Berkowitz, M. L.; Darden, T.; Lee, H.; Pedersen, L. G. *J. Chem. Phys.* **1995**, *103*, 8577–8593.

(10) Yeh, I.-C.; Berkowitz, M. L. *J. Chem. Phys.* **1999**, *111*, 3155–3162.

(11) Shimizu, K.; Freitas, A. A.; Atkin, R.; Warr, G. G.; FitzGerald, P. A.; Doi, H.; Saito, S.; Ueno, K.; Umebayashi, Y.; Watanabe, M.; Canongia Lopes, J. N. *Phys. Chem. Chem. Phys.* **2015**, *17*, 22321–22335.

(12) Chaban, V. *Phys. Chem. Chem. Phys.* **2011**, *13*, 16055–16062.

(13) Fedorov, M. V.; Lynden-Bell, R. M. *Phys. Chem. Chem. Phys.* **2012**, *14*, 2552–2556.

(14) Ivaništšev, V.; O'Connor, S.; Fedorov, M. V. *Electrochem. Commun.* **2014**, *48*, 61–64.

(15) Ivaništšev, V.; Fedorov, M. V. *Electrochem. Soc. Interface* **2014**, *23*, 65–69.

(16) Canongia Lopes, J. N.; Pádua, A. A. H. *J. Phys. Chem. B* **2004**, *108*, 16893–16898.

(17) Jorgensen, W. L.; Maxwell, D. S.; Tirado-Rives, J. *J. Am. Chem. Soc.* **1996**, *118*, 11225–11236.